Acta Crystallographica Section D
Biological Crystallography
ISSN 0907-4449

Interaction partners of PSD-93 studied by X-ray crystallography and fluorescence polarization spectroscopy

Monica Fiorentini, Anders Bach, Kristian Strømgaard, Jette S. Kastrup and Michael Gajhede

Department of Drug Design and Pharmacology, Faculty of Health and Medical Sciences, University of Copenhagen, Universitetsparken 2, DK-2100 Copenhagen, Denmark

Received 27 September 2012
Accepted 24 December 2012

PDB Reference: PSD-93 PZ1ext, 4h11

PSD-93 (chapsyn-110, DLG2) is a member of the family of membrane-associated guanylate kinase (MAGUK) proteins. The MAGUK proteins are involved in receptor localization and signalling pathways. The best characterized MAGUK protein, PSD-95, is known to be involved in NMDA receptor signalling *via* its PDZ domains. The PDZ domains of PSD-95 and PSD-93 are structurally very similar, but relatively little is known about the function of PSD-93. PSD-93 has been suggested to interact with GluD2 from the family of ionotropic glutamate receptors. Here, the interactions of four residues (GTSI) representing the extreme C-terminus of GluD2 with PSD-93 PDZ1 have been investigated in the crystalline phase. Two different binding modes of these residues were observed, suggesting that the peptide is not tightly bound to PSD-93 PDZ1. In accordance, the two N-terminal PSD-93 PDZ domains show no appreciable binding affinity for a GluD2-derived C-terminal octapeptide, whereas micromolar affinity was observed for a GluN2B-derived C-terminal octapeptide. This indicates that if present, the interactions between GluD2 and PSD-93 involve more than the extreme terminus of the receptor. In contrast, the tumour-suppressor protein SCRIB PDZ3 shows low micromolar affinity towards the GluD2-derived octapeptide, which is in agreement with previous findings using high-throughput assays.

1. Introduction

Membrane-associated guanylate kinases (MAGUKs) are proteins that play key roles in cell–cell intercommunication. They act as scaffold elements of surface complexes containing receptors, adhesion proteins and various signalling molecules. The members of the MAGUK family include PSD-93 (DLG2, chapsyn-110), PSD-95 (DLG4, SAP90), SAP97 (DLG1) and SAP102 (DLG3) (Funke *et al.*, 2005). All MAGUK proteins contain three N-terminal PDZ domains (PDZ1, PDZ2 and PDZ3), an Src homology 3 (SH3) domain and a guanylate kinase (GUK) domain (Kistner *et al.*, 1995). In several signalling pathways the MAGUK proteins function in cell–cell communication through interaction with other proteins. Most interactions are mediated by the PDZ domains, which are specialized protein–protein interaction domains (De Mendoza *et al.*, 2010).

PDZ domains generally bind short peptide motifs at the extreme C-terminus of receptors and ion channels. They consist of 80–90 amino-acid residues (Harrison, 1996; Pawson & Nash, 2003), and the entire family of PDZ domains has previously been divided into four classes based on the C-terminal sequences of their binding partners. For example, class I has a consensus binding sequence of *X*-[S/T]-*X*-φ, as found in NMDA receptors and in the metabotropic glutamate

receptor mGluR5. Recent investigations have shown that this classification scheme is probably too simple (Stiffler *et al.*, 2007). In 2008, Tonikian and coworkers reclassified PDZs into 16 classes on the basis of sequence recognition of the last eight residues (Tonikian *et al.*, 2008). The PDZ domains of MAGUK proteins are known to interact with the C-termini of ionotropic glutamate receptors (iGluRs). The most studied MAGUK protein, PSD-95, binds to the GluN2A and GluN2B subtypes of NMDA receptors (Lim *et al.*, 2002; Stiffler *et al.*, 2007).

Three-dimensional structures of the first two PSD-95 PDZ domains have been determined by X-ray crystallography and NMR (Tochio *et al.*, 2000; Long *et al.*, 2003); furthermore, the structure of a complex between PSD-95 PDZ3 and a class I peptide (TKNTKQTSV) has established a canonical binding mode (Doyle *et al.*, 1996). Using the fluorescence polarization technique, K_i values in the low micromolar range were observed between a GluN2B-derived C-terminal peptide and PSD-95 PDZ1 and PDZ2 (18 and 4 μM, respectively), whereas no appreciable binding affinity towards the PDZ3 domain was observed (Bach *et al.*, 2008). A slightly improved K_i value towards the GluN2B peptide was observed when using a tandem construct comprising both PDZ1 and PDZ2 of PSD-95.

PSD-93 is very similar to PSD-95 in terms of primary sequence (60% sequence identity between the full-length murine enzymes) and domain organization. Both proteins are expressed in the cerebellum in the post-synaptic regions between parallel fibres and Purkinje cells. However, a specific function for PSD-93 has still not been elucidated, and PSD-93 is mostly considered to be a redundancy system for other MAGUKs, *e.g.* PSD-95 (McGee *et al.*, 2001). Cerebellar Purkinje cells are enriched in PSD-93 (Cheng *et al.*, 2006) and also in GluD2 from the iGluR family (Zhao *et al.*, 1997). In 1999, Roche and coworkers demonstrated binding between GluD2 and the first two PDZ domains of both PSD-93 and PSD-95 using yeast two-hybrid techniques and immunoprecipitation (Roche *et al.*, 1999). In a chip-based study covering all cell membrane receptor C-terminal regions, interactions between GluD2 and PDZ3 of protein scribble homologue (SCRIB/ScrB1/LAP4), between GluD2 and PDZ1 of high-temperature requirement A serine peptidase (HtrA/serine protease HTRA1/L56/serine protease 11) and between GluD2 and PDZ1 of mitochondrial outer membrane protein 25 (OMP25/synaptojanin-2-binding protein/activin receptor-interacting protein 2/activin receptor-interacting protein 4) were reported (Stiffler *et al.*, 2007). However, binding between GluD2 and PDZ2 and PDZ3 of PSD-93 could not be demonstrated in the same study, pointing towards a role of PSD-93 PDZ1 in binding GluD2.

The binding pockets of PSD-93 PDZ1 and PSD-95 PDZ1 have previously been compared (Fiorentini *et al.*, 2009). It was shown that the two binding clefts were very similar, but that the binding cavity in PSD-95 was narrower than that in PSD-93. This suggested that the PDZ1 domain of PSD-93 might accept peptides with larger residues at the C-terminus than that of PSD-95, for example the GluD2 C-terminal Ile *versus* the Val found at the C-terminus of NMDA receptors. In this study, we have investigated interactions between PSD-93 PDZ domains and two peptides mimicking the C-terminal tails of GluD2 and GluN2B *in vitro* using fluorescence polarization spectroscopy and X-ray crystallography.

2. Materials and methods

2.1. Construct design and subcloning

To define the boundaries of the PSD-93 PDZ1 and PDZ2 domains, structural alignments were performed using the program *T-Coffee* (O'Sullivan *et al.*, 2004). PSD-93 PDZ1 and PDZ2 as defined in the PFAM database were extended by ten residues at each end. The domains were individually aligned with 15 PDZ domains of known structure in the *T-Coffee* regular Expresso mode. The boundaries were chosen to match those of the crystallized domains. In addition, constructs encoding PSD-93 PDZ1–2 and PSD-93 PDZ1 extended with the four extreme C-terminal residues (GTSI) of GluD2 (PSD-93 PDZ1ext) were designed. PSD-93 cDNA was obtained from Open Biosystems (Huntsville, Alabama, USA) as a synthetic mouse ORF from the Mammalian Gene Collection (Image Consortium Clone ID 100015000). The primers used for PCR cloning were as follows. PSD-93 PDZ1: forward primer, AAAGAATTCGAATTTGAAGAAATTACATTGGAGA; reverse primer, AAAAGCGGCCGCCTACCTTCTGCGCACGTACAGCC. PSD-93 PDZ1ext: forward primer, AAAGAATTCGAATTTGAAGAAATTACATTGGAGA; reverse primer, AAAGCGGCCGCTCATATGGACGTGCCCAATATGGGT. PSD-93 PDZ2: forward primer, AAAGAATTCACTGTTGTGG; reverse primer, AAAGCGGCCGCTCAAATAGTGGTC. PSD-93 PDZ1–2: forward primer, AAAGAATTCGAATTTGAAGAAATTACATTGGAGA; reverse primer, AAAAGCGGCCGCTCAAATAGTGGTGGGTTTGCCAA.

The amplified PCR products encoding residues 95–184 (PSD-93 PDZ1), residues 190–282 (PSD-93 PDZ2), residues 95–187 plus GTSI (PSD-93 PDZ1ext) and residues 95–282 (PSD-93 PDZ1–2) were subcloned into the *Eco*RI/*Not*I cloning sites of the pGEX-6P-1 plasmid (GE Healthcare, Hillerød, Denmark) using XL1-Blue supercompetent cells (Stratagene, La Jolla, California, USA) for transformation and selection of positive colonies. The constructs were verified by DNA sequencing (Eurofins MWG Operon, Germany).

The SCRIB PDZ3 boundaries were 986–1079 and were determined as described above for PSD-93. cDNA was obtained from Open Biosystems as for PSD-93. The primers for subcloning into the pOPIN vectors F and M using the high-throughput in-fusion system (Berrow *et al.*, 2009) were forward primer, AAGTTCTGTTTCAGGGCCCGTACCCTGTGGAGGAAATCTGCC, and reverse primer, ATGGTCTAGAAAGCTTTATGGGTCCCTCCGCACAAGCAGA.

2.2. Protein production and purification

Plasmid DNAs of PSD-93 PDZ domains were transformed into *Escherichia coli* BL21 (DE3) pLysS cells (Novagen;

Merck Biosciences, Darmstadt, Germany). When the culture reached an OD_{600} of 0.6 in LB medium, induction was carried out overnight at 310 K by adding 0.5 m*M* IPTG (Apollo Scientific, Tokyo, Japan). The proteins were produced as GST-fusion proteins and were purified by affinity chromatography after cell disruption (Constant Systems Ltd, England) using a GSTrap FF affinity column (GE Healthcare). The affinity tag was removed by overnight incubation at 277 K with 3C protease (1 U per milligram of fusion protein), leaving eight N-terminal residues (GPLGSPEF) from the tag-linker region. The proteins were further purified by size-exclusion chromatography (Superdex 75 HR, GE Healthcare) in PBS buffer (140 m*M* NaCl, 2.7 m*M* KCl, 10 m*M* Na_2HPO_4, 1.8 m*M* KH_2PO_4 pH 7.3). Finally, PSD-93 PDZ-containing fractions were concentrated by centrifugal filtration (Amicon Ultra-4) to obtain the final concentrations used in subsequent experiments. The purity of the samples was checked by SDS–PAGE.

Plasmid DNA of the SCRIB protein was introduced into *E. coli* BL21 (DE3) cells (Novagen). Expression was carried out in ZYM-5052 medium (auto-induction medium; Studier, 1991). When the culture density started to increase (4 h after inoculation), the temperature was lowered from 310 to 293 K and the expression culture was left overnight. The protein was produced as a His-fusion protein and was purified by affinity chromatography using a HisTrap FF affinity column (GE Healthcare) after cell disruption (Constant Systems Ltd). The affinity tag was removed by overnight incubation at 277 K with 3C protease (1 U per milligram of fusion protein). The protein was further purified by size-exclusion chromatography (Superdex 75 HR, GE Healthcare) and ion-exchange chromatography (5 ml cation-exchange column, GE Healthcare) in 20 m*M* sodium acetate pH 5.0, 10 m*M* EDTA. The purity of the samples was checked by SDS–PAGE.

2.3. Fluorescence polarization spectroscopy

The fluorescence polarization (FP) of all samples was measured using a Safire2 plate reader (Tecan, Switzerland). All measurements were performed in triplicate. The fluorescent probes used were the peptide LSSIESDV corresponding to the extreme C-terminus of GluN2B with a cyanine Cy5 fluorophore attached (Cy5-GluN2B) and the peptide DPDRGTSI corresponding to the extreme C-terminus of GluD2 with Cy5 attached (Cy5-GluD2). The excitation and emission wavelengths were 649 and 670 nm, respectively. To measure the binding affinity (i) between Cy5-GluN2B and PSD-93 PDZ1, PDZ2 and PDZ1–2 and (ii) between Cy5-GluD2 and PSD-93 PDZ1, PDZ2 and PDZ1–2, saturation binding experiments were performed. A fixed concentration of labelled peptides (50 n*M*) and increasing concentrations of PDZs were used: PDZ1, twofold dilution series from 500 to 0.24 µ*M*; PDZ2, from 250 to 0.1 µ*M*; PDZ1–2, from 61.2 to 0.02 µ*M*. Before measurements, the *g*-factor was adjusted so that 50 n*M* labelled peptide without any PDZ present would give an FP value of 20 mP. The assay was performed in PBS buffer. Each PDZ domain was incubated with the labelled peptides for 10 min before measurement.

Table 1
Crystal data and data-collection and refinement statistics.

Values in parentheses are for the outer resolution bin.

Data collection	
X-ray source	Synchrotron radiation
Wavelength (Å)	1.0
Space group	$P2_12_12_1$
Unit-cell parameters (Å)	a = 33.20, b = 45.55, c = 104.24
Resolution (Å)	28–1.67 (1.73–1.67)
No. of unique observations	18859 (2673)
Completeness (%)	99.2 (99.8)
Average multiplicity	5.8 (5.8)
$\langle I/\sigma(I)\rangle$	4.7 (2.0)
$R_{\rm merge}$† (%)	0.102 (0.364)
Wilson B (Å^2)	17.0
Refinement	
R‡ (%)	0.171
$R_{\rm free}$§ (%)	0.214
No. of residues	
Molecule *A*	102
Molecule *B*	102
No. of waters	187
No. of sulfates	1
No. of acetates	1
R.m.s.d. from ideal bond lengths¶ (Å)	0.010
R.m.s.d. from ideal bond angles¶ (°)	1.2
Mean B factor (Å^2)	
Molecule *A*	25.8
Molecule *B*	30.6
Water	33.7
Sulfate	47.2
Acetate	55.6
Ramachandran outliers†† (%)	0
Ramachandran favoured†† (%)	96
Rotamer outliers†† (%)	2.3
C^β outliers†† (%)	0
Clashscore††	10.2

† A measure of agreement among multiple measurements of the same reflections, $R_{\rm merge}$ is calculated as $\sum_{hkl}\sum_i |I_i(hkl) - \langle I(hkl)\rangle|/\sum_{hkl}\sum_i I_i(hkl)$, where $I_i(hkl)$ is the intensity of an individual measurement of the reflection with Miller indices hkl and $\langle I(hkl)\rangle$ is the average intensity from multiple observations. ‡ $R = \sum_{hkl}\big||F_{\rm obs}| - |F_{\rm calc}|\big|/\sum_{hkl}|F_{\rm obs}|$, where $F_{\rm obs}$ and $F_{\rm calc}$ are the observed and calculated structure-factor amplitudes, respectively. § The free R factor, $R_{\rm free}$, is computed in the same manner as R but using only a small set (5%) of randomly chosen intensities that were not used in the refinement of the model. ¶ Ideal bond lengths and angles were taken from Engh & Huber (1991). †† *MolProbity* statistics (Chen *et al.*, 2010).

To measure the binding affinity between Cy5-GluN2B or Cy5-GluD2 and SCRIB, saturation binding experiments were performed. A fixed concentration of labelled peptides (50 n*M*) and increasing concentrations of SCRIB (twofold dilution series from 60 to 0.02 µ*M*) were used. The measurement procedure was the same as for the PSD-93 domains.

2.4. Protein crystallization, structure determination and refinement

Crystallization of PSD-93 PDZ1ext was performed using the hanging-drop vapour-diffusion technique by mixing 1 µl of a 2 mg ml^{-1} protein solution in PBS buffer and 1 µl reservoir solution (0.2 *M* lithium sulfate, 20% PEG 1000, 0.1 *M* citric acid/sodium hydrogen phosphate pH 4.2). The reservoir volume was 500 µl. Crystals were obtained at room temperature within 2 d. Cryoprotection of the crystal was obtained by the addition of 20% sucrose to the reservoir solution.

X-ray data were collected at 100 K using synchrotron radiation at MAX-lab, Lund, Sweden. The data were indexed,

integrated and scaled using the *CCP*4 programs *MOSFLM* and *SCALA* (Winn *et al.*, 2011). The structure was determined by the molecular-replacement method using the program *Phaser* (McCoy *et al.*, 2007). The crystal structure of PSD-93 PDZ1 (PDB entry 2wl7; Fiorentini *et al.*, 2009) was used as the search model and a convincing solution accounting for the two molecules in the asymmetric unit was obtained.

Subsequently, automated model building was performed using the program *ARP*/*wARP* (Langer *et al.*, 2008). Missing residues were inserted manually using the program *Coot* (Emsley *et al.*, 2010). Structure refinement was performed with the *PHENIX* program package (Adams *et al.*, 2011) using TLS, isotropic *B* factors and riding H atoms. Water molecules were gradually introduced into the structure. All residues except for the four N-terminal residues (Gly-Pro-Leu-Gly) of the tag-linker region could be modelled. The quality of the structure was evaluated using the program *PROCHECK* (Laskowski *et al.*, 1996). Figures were prepared with the program *PyMOL* (Schrödinger; http://www.pymol.org).

The coordinates and structure factors have been deposited in the Protein Data Bank (Berman *et al.*, 2000; http://www.pdb.org) with accession code 4h11.

3. Results and discussion

3.1. Crystal structure of PSD-93 PDZ1ext

The crystal structure of PSD-93 PDZ1ext was determined to 1.67 Å resolution with two molecules (*A* and *B*) in the asymmetric unit of the crystal. Crystal data and data-collection and refinement statistics are listed in Table 1. All of the residues except for Asn154 are in allowed regions of the Ramachandran plot (91.0% of the residues are in most favoured regions, 7.8% are in additional allowed regions, 0.6% are in generously allowed regions and 0.6% are in disallowed regions). However, Asn154 is well defined in both molecules (Fig. 1).

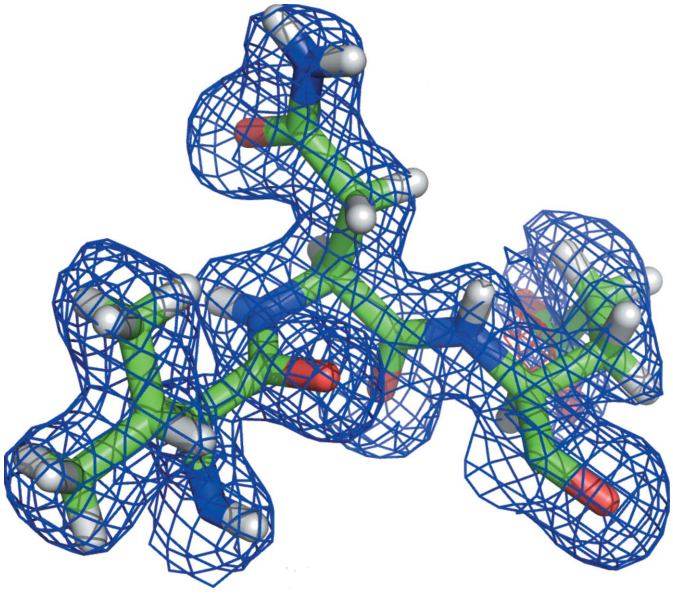

Figure 1
Representative $2mF_o - DF_c$ electron density of residues in the vicinity of Asn154. The map is contoured at 0.77 e Å^{-3}.

Each molecule comprises five β-strands and two α-helices (Fig. 2). The β-strands form a β-sandwich, with one strand participating in both sheets. In both molecules, the GTSI extension binds in the binding cleft of a symmetry-related molecule (*e.g.* GTSI of molecule *A* binds in the binding site of a symmetry-related molecule *A*; Fig. 3*a*). Overall, the two molecules of the asymmetric unit are very similar and superimpose with an r.m.s.d. of 0.18 Å on 78 C$^{\alpha}$ atoms. However, the C-terminal region linking the GTSI extension is highly flexible as deduced from the *B* values of the structure (Fig. 4). Also, the GTSI extensions have higher *B* values than the binding-site residues.

The binding grooves are not identical in the two molecules. A significant difference in the conformation of the loop connecting βA and βB is observed (Fig. 2), making the peptide-binding cleft of molecule *B* somewhat wider than that of molecule *A*. This difference in loop conformation is most likely to arise from different crystal-packing environments of the loop in molecules *A* and *B*, respectively. In molecule *A*, the side chain of Asn105 forms contacts to a water molecule, Arg152 and Glu155 of a symmetry-related molecule *A*. A different network of interactions from Asn105 is observed in molecule *B*. Here, the side chain of Asn105 makes contacts to two water molecules and to the side chain of Ser(−1) of the GTSI extension (numbered from −3 to 0 starting from the C-terminal isoleucine) of a symmetry-related molecule *A*.

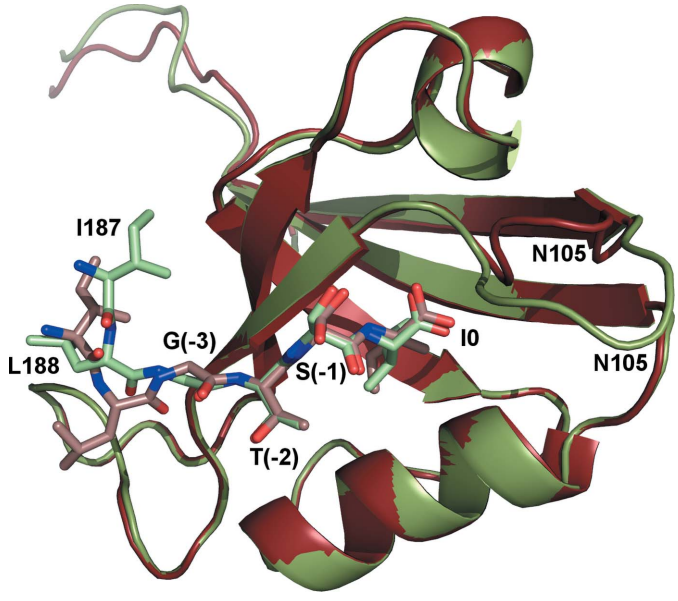

Figure 2
Structure of PSD-93 PDZ1 with a C-terminal GTSI extension to mimic the C-terminal tail of the glutamate receptor GluD2. The two molecules of PSD-93 PDZ1ext found in the asymmetric unit of the crystal have been superimposed. Molecule *A* is shown in brown and molecule *B* is shown in green. The bound GTSI extensions of symmetry-related molecules are shown in lighter corresponding colours. The residues of the GTSI extension are labelled from (−3) to 0. Each molecule shows the well known PDZ-domain structure containing seven segments of secondary structure (five β-strands and two α-helices).

The PDZ–peptide interactions observed in both molecules of PSD-93 PDZ1 are similar to those observed in a multitude of other PDZ–peptide complexes (Kornau *et al.*, 1995; Harrison, 1996; Niethammer *et al.*, 1996). In the binding cleft of molecule *A*, polar interactions are observed between the carboxylate group of Ile0 and the main-chain N atoms of Leu108, Gly109 and Phe110 as well as to one water molecule (W1; Fig. 3*b*). This water molecule is not observed in molecule *B*. The amide N atom of Ile0 forms a hydrogen bond to the backbone carbonyl O atom of Phe110. The side chain of Ser(−1) is observed in two conformations, forming primarily water-mediated interactions (W2 and W3). The only hydrogen bond to the αB helix occurs between the hydroxyl O atom of Thr(−2) and the $N^{\varepsilon 3}$ atom of His163. The residues of the GTSI extension are also engaged in the formation of conventional β-sheet hydrogen bonds to Ile112 in the βB strand of the PDZ1 domain.

The different topologies of the binding clefts lead to a different binding mode of the C-terminal Ile0 of molecule *B*

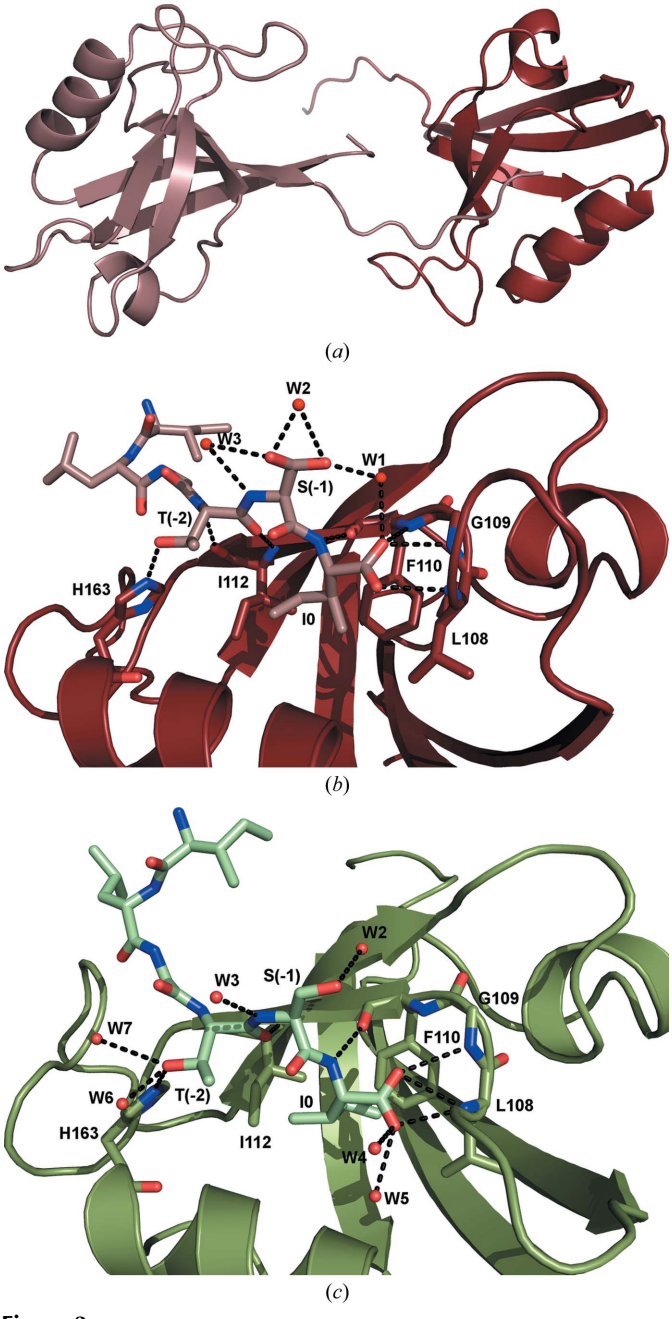

(*a*) (*b*) (*c*)

Figure 3
Binding mode of the C-terminal GTSI extension to PSD-93 PDZ1. (*a*) In both molecule *A* and molecule *B* the GTSI extension binds in the binding cleft of a symmetry-related molecule (*e.g.* GTSI of molecule *A* binds in the binding site of a symmetry-related molecule *A*). Only molecule *A* (brown) and a symmetry-related molecule *A* (lighter brown) are shown. (*b*, *c*) Potential hydrogen-bonding interactions (stippled lines) between the GTSI extensions and PSD-93 PDZ1ext. (*b*) Interactions between molecule *A* and the GTSI extension of a symmetry-related molecule *A*. (*c*) Interactions between molecule *B* and the GTSI extension of a symmetry-related molecule *B*.

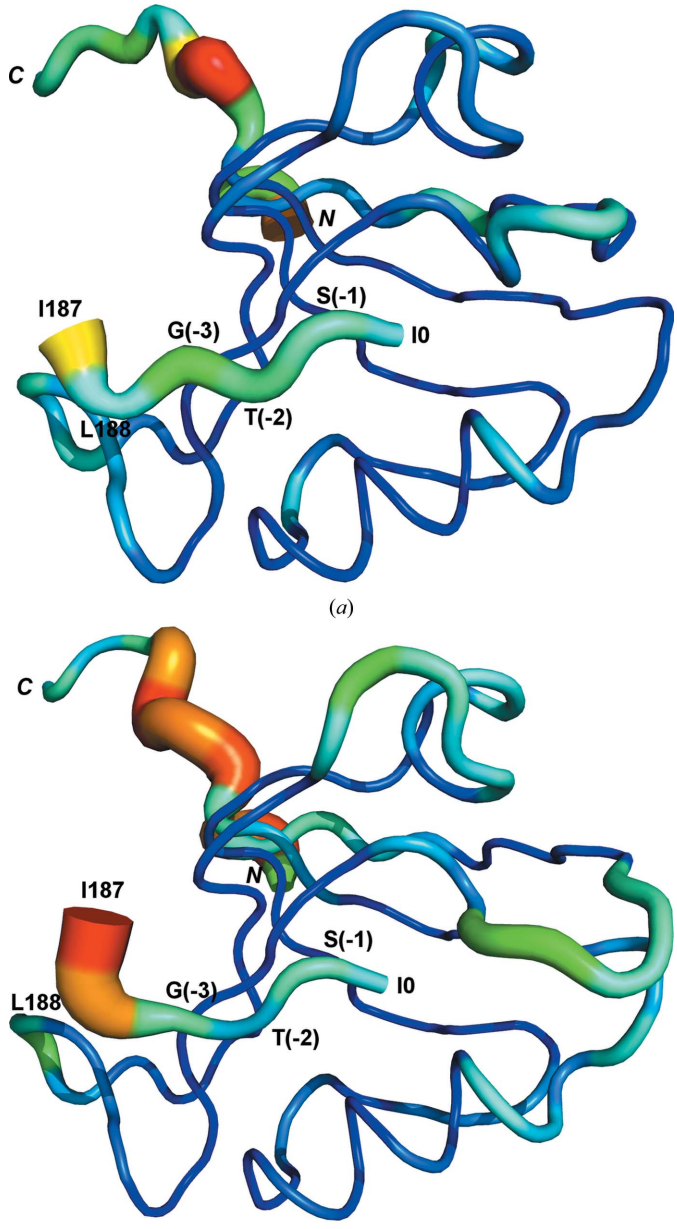

(*a*) (*b*)

Figure 4
Flexibility of PSD-93 PDZ1ext. The *B* values of molecule *A* (*a*) and molecule *B* (*b*) are shown in '*B*-factor putty mode' in *PyMOL*, with the highest *B* values (110 Å^2) coloured red and the lowest *B* values (6 Å^2) coloured blue.

Table 2
Binding affinity of GluD2- and GluN2B-derived peptides to PSD-93 PDZ domains.

n.d., not determined.

PDZ domain	Peptide	K_d† (μM)	B_{max} (mP)
PSD-93 PDZ1	Cy-GluN2B	19.2 ± 1.1	51.8 ± 0.8
	Cy-GluD2	>500	n.d.
PSD-93 PDZ2	Cy-GluN2B	8.5 ± 0.6	50.7 ± 0.9
	Cy-GluD2	>250	n.d.
PSD-93 PDZ1–2	Cy-GluN2B	3.2 ± 0.2	77.2 ± 1.3
	Cy-GluD2	>61	n.d.
SCRIB PDZ3	Cy-GluD2	7.3 ± 1.4	17.1 ± 1.0

† K_d values from fluorescence polarization spectroscopy are shown as mean values with the mean standard error of the mean (SEM).

compared with molecule *A*. Owing to the altered conformation of the loop between the αB helix and the βB sheet in molecule *B*, the peptide is pushed further back into the cavity compared with molecule *A* (Fig. 3*c*). This leads to differences in the conformation of the Ile0 side chain and in the involvement of water molecules in binding. Two water molecules (W4 and W5) in molecule *B* are observed in the vicinity of Ile0 which are not present in the binding site of molecule *A*. The side chain of Ser(−1) is clearly defined in one conformation only and the hydroxyl group makes a hydrogen bond to one water molecule (W2). The other polar interactions observed in the binding groove of molecule *B* are similar to those seen in molecule *A*.

This structure has been compared with the previously reported structure of PSD-93 PDZ1 in the absence of a GluD2 peptide extension (Fiorentini *et al.*, 2009). Superposition of the *A* chains of the two structures gives an r.m.s.d. of 0.31 Å, and with the exception of the loop connecting βA and βB the structures are similar. The conformation of the loop in the previously reported structure makes the cleft even wider than it is in molecule *B* of the present structure.

In conclusion, the crystal structure of PSD-93 PDZ1ext supports the ability of the extreme C-terminal tail of GluD2 to form interactions with PSD-93 PDZ1. Although the GTSI extension binds with interactions similar to those observed in many other complexes involving PDZ domains, crystal-packing interactions can introduce two different binding modes of GTSI, suggesting that the peptide tail is not tightly bound.

3.2. Binding of the C-terminus of GluD2 to PDZ domains

To further investigate the binding properties of the C-terminal tail of GluD2 relative to the C-terminal tail of GluN2B, we performed binding studies using fluorescence polarization spectroscopy. The results of the saturation experiments with PSD-93 PDZ1, PDZ2 and PDZ1–2 are shown in Figs. 5(*a*), 5(*b*) and 5(*c*), and the derived equilibrium constants are provided in Table 2. The GluD2-derived peptide Cy-GluD2 showed no appreciable binding affinity to any of the PSD-93 constructs, whereas the GluN2B-derived peptide Cy-GluN2B showed binding affinity in the micromolar range. Cy-GluN2B binds to PSD-93 PDZ1 with a K_d of 19 μM and to PSD-93 PDZ2 with a K_d of 9 μM. The presence of both PSD-93 PDZ domains (PSD-93 PDZl–2) leads to a slight increase in the binding affinity of Cy-GluN2B (K_d = 3 μM). The K_d values obtained for the GluN2B-derived peptide are comparable to those obtained for similar constructs of PSD-95 (Lim *et al.*, 2002; Stiffler *et al.*, 2007) and PSD-93 PDZ2 (Stiffler *et al.*, 2007). This supports the previous findings that PSD-93, like PSD-95, is an interaction partner of the NMDA receptors (Niethammer *et al.*, 1996).

The binding affinities of the PSD-93 PDZ domains towards the Cy-GluD2 peptide were found to be at least two orders of magnitude lower compared with their affinities for Cy-GluN2B. Our findings suggest that PSD-93 does not exclusively interact with the extreme C-terminus of GluD2 and that interactions with other regions of the intracellular receptor part might be required to gain binding affinity. This is

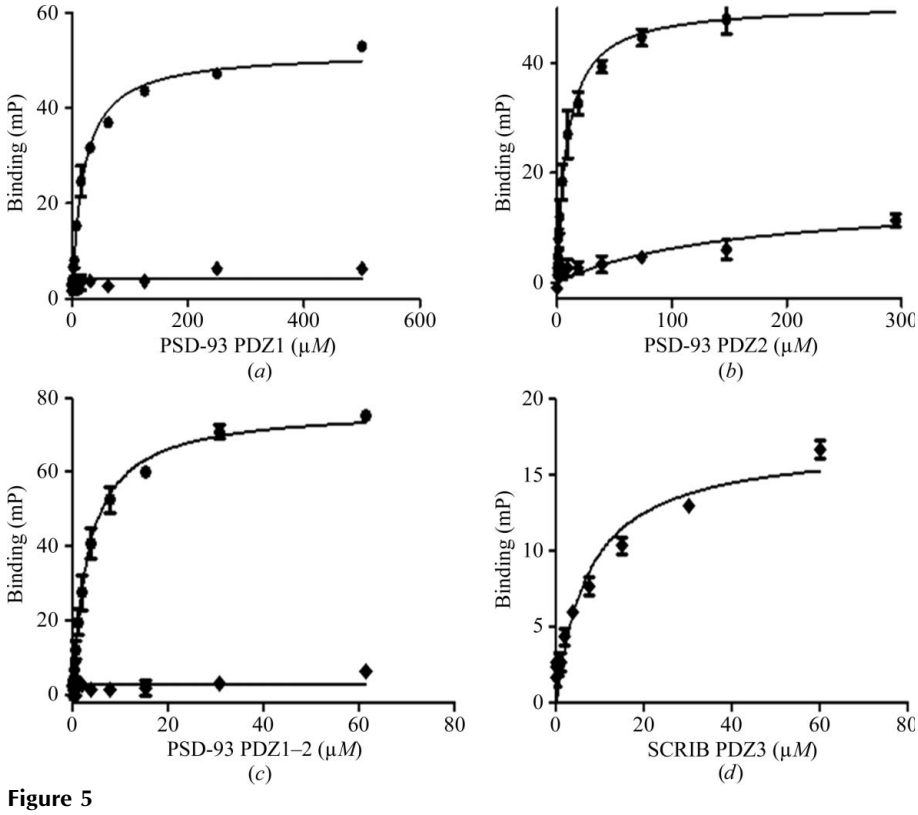

Figure 5
Saturation binding studies using fluorescence polarization spectroscopy. The experiments were carried out with Cy5-GluN2B (LSSIESDV; circles) or Cy5-GluD2 (DPDRGTSI; diamonds) octapeptides and PSD-93 PDZ domains (*a*, *b*, *c*) or SCRIB PDZ3 (*d*). All measurements were made in triplicate.

somewhat unanticipated, since PDZ-mediated interactions are usually considered to only include linear epitopes of lengths of up to 6–8 residues (Doyle *et al.*, 1996; Niethammer *et al.*, 1996; Lim *et al.*, 2002; Stiffler *et al.*, 2007; Tonikian *et al.*, 2008). Also, our *in vitro* findings do not support the *ex vivo* results reported previously, which showed that the first two PSD-93 PDZ domains (residues 83–421) interact with the C-terminus of GluD2 (residues 852–1008) and that mutations amongst the last four residues of GluD2 would disrupt the interaction (Roche *et al.*, 1999).

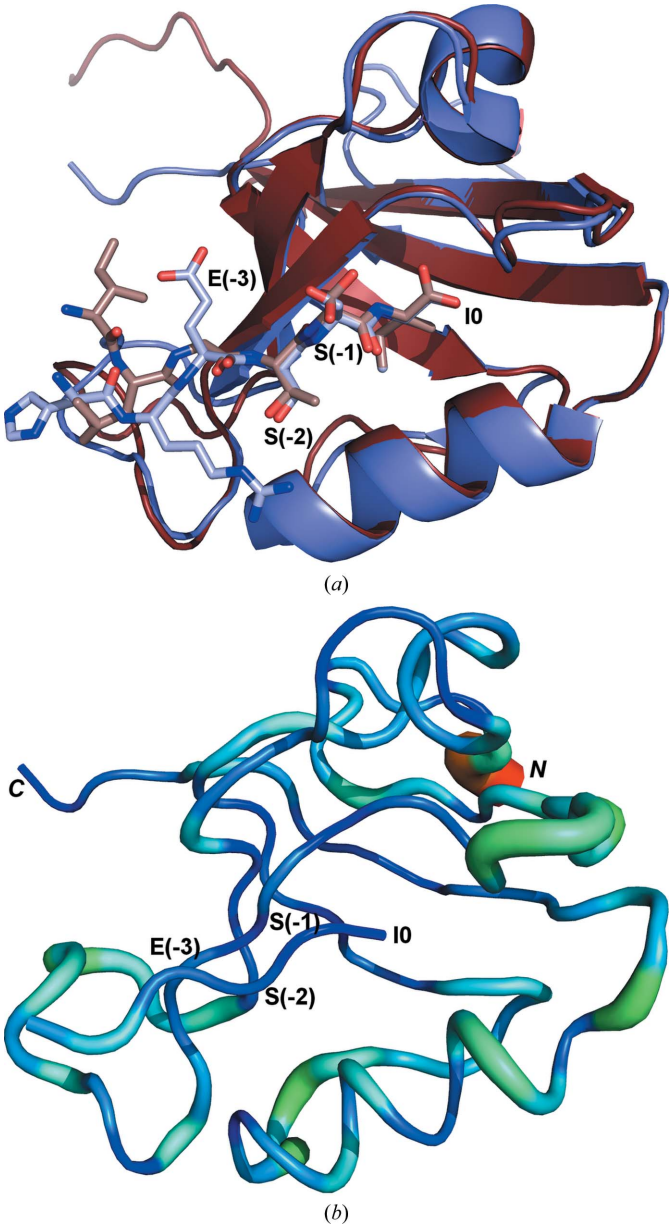

Figure 6
Structure of OMP25 PDZ1 with a C-terminal ESSI extension. (*a*) Superimposition of the structures of OMP25 PDZ1 (PDB entry 2jin, blue) and PSD-93 PDZ1ext (molecule *A*, brown), showing the similar binding mode of the ESSI extension in OMP25 and the GTSI extension in PSD-93 PDZ1. (*b*) The *B* values of OMP25 PDZ1 are shown in '*B*-factor putty mode' in *PyMOL*, with the highest *B* values (67 Å^2) coloured red and the lowest *B* values (10 Å^2) coloured blue.

The GluD2-derived peptide has previously been reported to bind to the PDZ3 domain of SCRIB in a high-throughput study (Stiffler *et al.*, 2007). Therefore, to demonstrate that the GluD2-derived peptide is capable of binding to PDZ domains, we performed saturation experiments with SCRIB PDZ3 (Fig. 5*d*). The K_d value was found to be 7 µ*M*, which is comparable with the K_d value from the high-throughput study and the values for Cy-GluN2B towards PSD-93 PDZ domains. Structures of SCRIB PDZ3 are not presently available. However, structures of OMP25 PDZ1 have recently been deposited in the Protein Data Bank (PDB entries 2jik and 2jin; J. Tickle, C. Phillips, A. C. W. Pike, C. Cooper, E. Salah, J. Elkins, A. P. Turnbull, A. Edwards, C. H. Arrowsmith, J. Weigelt, M. Sundstrom & D. Doyle, unpublished work) with a C-terminal ESSI extension. The ESSI extension binds to OMP25 in the same way as the GTSI extension in PSD93ext (Fig. 6*a*). However, the *B* values of the ESSI extension in OMP25 indicate that the tail is more stabilized in the binding site (Fig. 6*b*) compared with the GTSI extension in PSD-93 (Fig. 4). This difference might partly explain why a binding affinity of 8 µ*M* has been observed for GluD2 with PDZ1 of OMP25 (Stiffler *et al.*, 2007) and why very weak binding between the C-terminal tail of GluD2 and PSD-93 PDZ1 is found in this study. Based on the observation that OMP25 binds both GTSI and ESSI, it might be speculated that it is not important whether either Gly or Glu is present at position (−3), while Thr or Ser at position (−2) both form the same type of hydrogen bonds and Ser at position (−1) points outwards; therefore, Ile at position 0 seems to be important for binding to OMP25 PDZ1. When comparing amino acids in superimposed structures of PSD-93 PDZ1, PSD-95 PDZ1 and OMP25 PDZ1 in the immediate surroundings of Ile0, they are identical with one exception. The PSD-93 Leu170 is also Leu in PSD-95 but is Phe in OMP25. This substitution might be the reason why OMP25 PDZ1 but neither PSD-93 PDZ1 nor PSD-95 PDZ1 binds peptides derived from the C-terminal tail of GluD2 with appreciable binding affinity and why the GluN2B-derived peptide with Val at position 0 binds with high affinity to both PSD-93 and PSD-95.

4. Conclusion

The structure of PSD-93 PDZ1 with a C-terminal GTSI extension to mimic the C-terminal tail of GluD2 shows flexibility in the binding cavity, resulting in variations in GTSI binding. Combined with the very low binding affinity of a GluD2-derived peptide to PSD-93 PDZ1, PDZ2 and PDZ1–2, this suggests that (i) PSD-93 does not exclusively interact with the C-terminal tail of GluD2 and that interactions with other regions of the C-terminal region are required to gain binding affinity or (ii) that PSD-93 is not a primary interaction partner of GluD2. PSD-93 binds a GluN2B-derived peptide with comparable binding affinity as previously reported for PSD-95. Therefore, it cannot be excluded that PSD-93 may be a redundancy system for, for example, PSD-95.

The University of Copenhagen Programme of Excellence (GluTarget) and DanScatt are acknowledged for support. Diffraction data were collected at the MAX-lab synchrotron facility, Lund, Sweden. Mrs Heidi Peterson is thanked for technical assistance.

References

Adams, P. D. *et al.* (2011). *Methods*, **55**, 94–106.

Bach, A., Chi, C. N., Olsen, T. B., Pedersen, S. W., Røder, M. U., Pang, G. F., Clausen, R. P., Jemth, P. & Strømgaard, K. (2008). *J. Med. Chem.* **51**, 6450–6459.

Berman, H. M., Westbrook, J., Feng, Z., Gilliland, G., Bhat, T. N., Weissig, H., Shindyalov, I. N. & Bourne, P. E. (2000). *Nucleic Acids Res.* **28**, 235–242.

Berrow, N. S., Alderton, D. & Owens, R. J. (2009). *Methods Mol. Biol.* **498**, 75–90.

Chen, V. B., Arendall, W. B., Headd, J. J., Keedy, D. A., Immormino, R. M., Kapral, G. J., Murray, L. W., Richardson, J. S. & Richardson, D. C. (2010). *Acta Cryst.* D**66**, 12–21.

Cheng, D., Hoogenraad, C. C., Rush, J., Ramm, E., Schlager, M. A., Duong, D. M., Xu, P., Wijayawardana, S. R., Hanfelt, J., Nakagawa, T., Sheng, M. & Peng, J. (2006). *Mol. Cell. Proteomics*, **5**, 1158–1170.

Doyle, D. A., Lee, A., Lewis, J., Kim, E., Sheng, M. & MacKinnon, R. (1996). *Cell*, **85**, 1067–1076.

Emsley, P., Lohkamp, B., Scott, W. G. & Cowtan, K. (2010). *Acta Cryst.* D**66**, 486–501.

Engh, R. A. & Huber, R. (1991). *Acta Cryst.* A**47**, 392–400.

Fiorentini, M., Nielsen, A. K., Kristensen, O., Kastrup, J. S. & Gajhede, M. (2009). *Acta Cryst.* F**65**, 1254–1257.

Funke, L., Dakoji, S. & Bredt, D. S. (2005). *Annu. Rev. Biochem.* **74**, 219–245.

Harrison, S. C. (1996). *Cell*, **86**, 341–343.

Kistner, U., Garner, C. C. & Linial, M. (1995). *FEBS Lett.* **359**, 159–163.

Kornau, H. C., Schenker, L. T., Kennedy, M. B. & Seeburg, P. H. (1995). *Science*, **269**, 1737–1740.

Langer, G., Cohen, S. X., Lamzin, V. S. & Perrakis, A. (2008). *Nature Protoc.* **3**, 1171–1179.

Laskowski, R. A., Rullmannn, J. A., MacArthur, M. W., Kaptein, R. & Thornton, J. M. (1996). *J. Biomol. NMR*, **8**, 477–486.

Lim, I. A., Hall, D. D. & Hell, J. W. (2002). *J. Biol. Chem.* **277**, 21697–21711.

Long, J.-F., Tochio, H., Wang, P., Fan, J.-S., Sala, C., Niethammer, M., Sheng, M. & Zhang, M. (2003). *J. Mol. Biol.* **327**, 203–214.

McCoy, A. J., Grosse-Kunstleve, R. W., Adams, P. D., Winn, M. D., Storoni, L. C. & Read, R. J. (2007). *J. Appl. Cryst.* **40**, 658–674.

McGee, A. W., Topinka, J. R., Hashimoto, K., Petralia, R. S., Kakizawa, S., Kauer, F. W., Aguilera-Moreno, A., Wenthold, R. J., Kano, M., Bredt, D. S. & Kauer, F. (2001). *J. Neurosci.* **21**, 3085–3091.

Mendoza, A. de, Suga, H. & Ruiz-Trillo, I. (2010). *BMC Evol. Biol.* **10**, 93.

Niethammer, M., Kim, E. & Sheng, M. (1996). *J. Neurosci.* **16**, 2157–2163.

O'Sullivan, O., Suhre, K., Abergel, C., Higgins, D. G. & Notredame, C. (2004). *J. Mol. Biol.* **340**, 385–395.

Pawson, T. & Nash, P. (2003). *Science*, **300**, 445–452.

Roche, K. W., Ly, C. D., Petralia, R. S., Wang, Y.-X., McGee, A. W., Bredt, D. S. & Wenthold, R. J. (1999). *J. Neurosci.* **19**, 3926–3934.

Stiffler, M. A., Chen, J. R., Grantcharova, V. P., Lei, Y., Fuchs, D., Allen, J. E., Zaslavskaia, L. A. & MacBeath, G. (2007). *Science*, **317**, 364–369.

Studier, F. W. (1991). *J. Mol. Biol.* **219**, 37–44.

Tochio, H., Hung, F., Li, M., Bredt, D. S. & Zhang, M. (2000). *J. Mol. Biol.* **295**, 225–237.

Tonikian, R. *et al.* (2008). *PLoS Biol.* **6**, e239.

Winn, M. D. *et al.* (2011). *Acta Cryst.* D**67**, 235–242.

Zhao, H.-M., Wenthold, R. J., Wang, Y.-X. & Petralia, R. S. (1997). *J. Neurochem.* **68**, 1041–1052.